

# AN INNOVATIVE PROCEDURE TO COMPUTE EQUIVALENT BLOCK SIZE IN A DUAL-POROSITY MODEL

S. SARDA, B.J. BOURBIAUX, M.C. CACAS and J.C. SABATHIER  
Institut Français du Pétrole, PO Box 311, 92506 Rueil-Malmaison, France

## Introduction

In recent years, new techniques and methods have been developed to characterize the natural fracturing at various field scale and integrate fractured reservoir characterization data into 3D geometrical models of fracture networks. However, 3D images of fractured reservoir are not directly usable as a reservoir simulation input. Representing the fracture network in reservoir flow simulators was always considered unrealistic because of the partial knowledge of this network and because of numerical limitations. Actually, the Warren & Root model<sup>1</sup> remains the basis for any dual porosity simulator. In this model, the fractured reservoir is represented as an array of numerical parallelepipedic matrix blocks separated by uniform orthogonal fractures.

To obtain reliable predictions from such a flow simulator, representative values of fracture and matrix petrophysical properties and of equivalent block dimensions have to be assigned to each cell of the flow simulator. But the equivalent fracture permeability and the dimensions of numerical blocks cannot be directly derived from the observation of geological images. Hence, a methodology and a software have been developed to compute the parameters of dual porosity simulators from fractured reservoir images<sup>2</sup>. In this paper, we develop the methodology used for the equivalent block determination. Then, validation cases are presented as well as the application of this procedure to a complex fracture network.

## Methodology

The input of this method is a 3D fractured reservoir image representing a naturally fractured reservoir. This image is a parallelepipedic volume discretized vertically as a list of layers. Fractures are assumed to be perpendicular to bed limits. Hence, the matrix blocks are not limited by fracture planes in the vertical direction and no vertical dimension of equivalent blocks needs to be determined. The method described hereafter enables to compute the horizontal dimensions of equivalent blocks for each layer of the image and for several layers lumped together.

The identification of the equivalent horizontal dimensions of numerical matrix blocks in a layer is based on the water-oil capillary imbibition mechanism. For an oil saturated matrix block surrounded with water, the capillary imbibition involves countercurrent flows of oil and water with a gradual advance of a smooth front from the boundaries to the centre of the block<sup>3</sup>. The dimensional analysis of the problem<sup>4</sup> shows that, for a one-dimensional flow in an infinite medium and for a given rock fluid system, the volume of water imbibed is proportional to the square root of time. Assuming a piston-type displacement, this means that the time necessary for the front to reach a given position  $x$  from the block limit imbibing water is proportional to  $x^2$ . Moreover, experimental studies<sup>5,6</sup> indicate that the time necessary to recover a given oil fraction from the block is roughly proportional to the square of sample length which is consistent with the dimensional analysis as long as the assumption of infinite acting flow behavior remains valid, that is, during the first stage of imbibition.

The problem addressed is that of finding the horizontal dimensions of the equivalent block for which the real fractured medium and the equivalent Warren & Root model give similar oil recovery functions  $R(t)$  and  $Req(t)$  for a water-oil capillary imbibition process in which water is initially present in fractures and oil in matrix blocks.

The geometrical method used to solve this problem is based on the following assumptions:

- The invasion of matrix by water is piston type.
- The function linking distance of water-oil front  $x$  from block boundaries and time  $t$  is independent of block shape for a given rock-fluid system. That is, if the matrix medium is isotropic and homogeneous, the same function  $x(t)$  is valid for all blocks.

Following the assumption of piston type flow, the recovery functions  $R(t)$  and  $Req(t)$  can be expressed as normalized invaded area functions  $A(t)$  and  $Aeq(t)$ . Furthermore, as the water front invasion kinetics is the same in all blocks,  $A(t)$  and  $Aeq(t)$  can be replaced by the functions  $A(x)$  and  $Aeq(x)$  which correspond to the normalized invaded area versus the distance between water front and block boundaries respectively in the real fractured layer and the equivalent Warren & Root model. The geometrical method consists in an

identification of the two functions  $A(x)$  and  $A_{eq}(x)$ .

The analytical expression of  $A_{eq}(x)$  is the following:

$$\left\{ \begin{array}{l} A_{eq}(a, b, x) = 1 - \frac{1}{ab}(a-2x)(b-2x) = 2\left(\frac{1}{a} + \frac{1}{b}\right)x - \frac{4}{ab}x^2, \quad x \in [0, \min(\frac{a}{2}, \frac{b}{2})] \\ A_{eq}(a, b, x) = 1, \quad x > \min(\frac{a}{2}, \frac{b}{2}) \end{array} \right.$$

$A(x)$  has no analytical expression. It is derived from a pixel type discretization of the XY layer section using an image processing algorithm. The number of pixels is generally more than 1 million. First, each fracture of the layer is codified on the image by initializing the corresponding pixels to 0. Other pixels are initialized to a value greater than the largest distance between two pixels. Second, a fast algorithm is used to compute, for each pixel of the image, the minimal distance between this pixel and the nearest fracture pixel. Then, a histogram is created by sorting the non zero distance values, which correspond to the matrix pixels, in increasing order (**Fig. 1**). The cumulated histogram gives, for a given distance value from fractures, the number of pixels which are closer from a fracture. Physically, this corresponds to the water invaded area versus the distance of water penetration. By dividing the cumulated histogram by the total number of non zero pixels (matrix pixels), we obtain the  $A(x)$  function.

The first derivative of  $A(x)$ ,  $A'(x)$ , is proportional to the water front perimeter. Consequently, the sign of  $A'(x)$  indicates if this water front perimeter is increasing or decreasing. **Fig. 2** shows a fractured layer section composed of small disconnected fractures. For such a layer, the water front perimeter is increasing during the first stage of imbibition and the corresponding  $A(x)$  function has a S shape. On the opposite, for a layer composed of connected fractures (**Fig. 3**), the water front perimeter is always decreasing. Note that in the Warren & Root model, the water front length is always decreasing for finite positive values of  $a$  and  $b$ . The identification of  $A(x)$  and  $A_{eq}(x)$  is performed by minimizing the following least square function:

$$J(a, b) = \sum_{i=1}^N (A(x_i) - A_{eq}(a, b, x_i))^2$$

The equivalent block dimensions are the values  $a$  and  $b$  for which the function  $J(a, b)$  is minimum.

In order to give the same weight to any volume of oil recovered whatever the time when it is produced, the  $A(x)$  curve is discretized with a constant area step along Y axis. The  $(x_i)$  series used in the expression of  $J(a, b)$  is inferred from this discretization. Hence, more weight is given to the parts of  $A(x)$  having the highest derivative values. Most often, it corresponds to the first stage of imbibition, when the water front perimeter is the longest.

Because  $a$  and  $b$  variables have symmetrical roles in the expression of  $A_{eq}(a, b, x)$ , another least square function is used:

$$\tilde{J}(u, v) = \sum_{i=1}^N (A(x_i) - \tilde{A}_{eq}(u, v, x_i))^2$$

$$\text{with } \left\{ \begin{array}{l} \tilde{A}_{eq}(u, v, x) = ux + vx^2 \\ \tilde{A}_{eq}(u, v, x) \leq 1 \end{array} \right. , \text{ and } u = 2\left(\frac{1}{a} + \frac{1}{b}\right), \quad v = \frac{-4}{ab}$$

The minimization of  $\tilde{J}(u, v)$  consists in finding the couple  $(\bar{u}, \bar{v})$  for which  $\tilde{J}'(\bar{u}, \bar{v}) = 0$ . This is done using a Newton algorithm.

Then, the couple  $(\bar{a}, \bar{b})$  is derived from  $(\bar{u}, \bar{v})$ . There are three cases:

- 1/  $\bar{v} > 0$ : One value of  $(\bar{a}, \bar{b})$  is negative, which is impossible. As  $\bar{v}$  has the sign of  $\tilde{A}_{eq}''(x)$ , the provided solution corresponds to an increasing water front length. This happens when the layer studied is composed of small disconnected fractures (**Fig. 2**). In such a case, the best estimated solution is obtained by imposing  $v=0$  in the expression of  $\tilde{A}_{eq}(u, v, x)$ . This corresponds to an infinite value of  $a$  or  $b$ , that is, to a set of infinitely-long parallel fractures, characterized by a constant water front length. The minimization process is then performed again and the couple  $(\bar{a}, \bar{b})$  is calculated as follows:

$$\bar{a} = \frac{2}{\bar{u}}, \quad \bar{b} \text{ infinite}$$

- 2/  $\bar{u}^2 + 4\bar{v} < 0$ :  $(\bar{a}, \bar{b})$  are not real values (complexes), which is impossible. In this case, the fitted normalized invaded area curve does not reach the line  $A_{eq}=1$ . This happens when the image section is made up of two sets of blocks characterized by well-differentiated dimensions. A complete fit of such an area-distance curve would be obtained with two equivalent blocks of different dimensions, however dual porosity simulators only take into account a single equivalent block per grid cell. The best compromise is obtained for a square block solution because the corresponding area-distance curve is tan-

gential to the line  $A_{eq}=1$ . Therefore, imposing  $u^2 + 4v = 0$ , the minimization process leads to:

$$\bar{a} = \bar{b} = \frac{4}{\bar{u}}$$

3/ For other couples  $(\bar{u}, \bar{v})$ , we have the general solution:

$$\bar{a}, \bar{b} = \frac{-\bar{u} \pm \sqrt{\bar{u}^2 + 4\bar{v}}}{\bar{v}}$$

The geometrical method is also valid to find the equivalent block dimensions of a stack of layers having the same petrophysical properties. In such a case, area-distance functions  $A_i(x)$  are computed for all the constitutive layers and the area-distance function  $A(x)$  referring to the whole stack is derived from the layer thicknesses  $H_i$  and area-distance functions  $A_i(x)$ :

$$A(x) = \sum_{i=1}^N H_i A_i(x)$$

Then, the minimization processed described above is performed with this new  $A(x)$  function.

### Validation

The geometrical method has been validated using a conventional single porosity two-phase flow simulator with the following procedure:

- The reference oil recovery function  $R(t)$  is computed with the conventional simulator on a finely discretized section of the real fractured block studied.
- The geometrical method is applied in order to find the equivalent block dimensions (a,b).
- The oil recovery function  $R_{eq}(t)$  is computed using the conventional simulator again on the equivalent block section of dimensions (a,b). Then,  $R(t)$  and  $R_{eq}(t)$  are compared.

The chosen rock-fluid data used in the two-phase flow simulator are the following: matrix porosity and permeability are equal to 0.3 and 1 mD, water and oil viscosities are equal to 0.35 and 0.43 cp. Relative permeability and capillary pressure data are given in **Table 1**. Other sets of data were also tested for validation and led to the same conclusions as those detailed hereafter.

Because the discretization of a fractured reservoir section involves a very high number of cells, we first validated the geometrical method on single blocks of various shapes: U-shaped, triangular, or comb-shaped blocks. These blocks are shown in **Fig. 4** with the square or rectangular equivalent block section in grey. For the U-shaped and triangular blocks, the imbibition curve referring to the equivalent block was very close to the reference curve. For the comb-shaped block, the recovery curves (**Fig. 6**) are exactly superimposed during the 10 to 20 first days and diverge afterwards despite a good fit between the area-distance curves referring to the comb-shaped block and the rectangular equivalent block (**Fig. 5**). Actually, due to the presence of connected internal fractures, the fronts advancing from two opposite fractures start interfering after 20 days and the assumption of infinite-acting flow behavior, underlying the geometrical method, is no more valid. Nevertheless, for fractured reservoir simulation purposes, this solution is reliable with regard to usual uncertainties.

We also considered a distribution of blocks assembled to build a fractured image section (**Fig. 7**). For this distribution, the reference recovery function was not directly computed with the two phase flow simulator but was determined from the solutions referring to the constitutive single blocks. **Fig. 8** shows the imbibition recovery curves referring to the distribution of blocks and the rectangular equivalent block. In this case, the slight difference observed is linked to the assumption that the front propagation kinetics is the same in all constitutive blocks. However, once again, this difference can be neglected if compared to other uncertainties inherent in fractured reservoir flow simulation.

### Application

The geometrical method has been applied to a large volume generated by our in-house stochastic fracture simulator. This image results from the integration of the fracturing data collected on a Devonian sandstone outcrop in Morocco. Its X,Y and Z dimensions are respectively 100 m, 100 m and 16.6 m (**Fig. 9**). It is made up of 9 geological layers of which thickness varies between 0.3 m for layer 7 and 5.8 m for layer 3. The fracture network includes 2 main fracture sets (regional systematic joints and fold related joints) oriented along the X and Y axis of the image. In a given layer, the fracture density is more or less proportional to the layer thickness. Hence, layers 3 and 7 (**Fig. 10** and **Fig. 11**) are respectively the least and most fractured layers.

Equivalent block dimensions were computed on 20 different subvolumes of the whole fractured block. These subvolumes include the 9 layers, have the same centre, and their areal dimensions vary from 5 m x 5 m to 100 m x 100 m with a 5 m step. This procedure enables to estimate a representative elementary volume (R.E.V.) for equivalent blocks.

The horizontal dimensions (a,b) of the equivalent block were determined for each individual layer and for

the 9 layers together. All computations were performed with the same linear definition of 22 pixels per meter, in order to allow comparison between the results obtained on different subvolumes. This definition corresponds to a number of pixels of 5 million for the whole image section. Note that with an Ultra-Spark 1-140 SUN Workstation, a layer discretized with 5 million pixels is processed in about 12 seconds CPU time. Whatever the subvolume and the layer considered, the geometrical method provided a square equivalent block solution.

**Fig 12** shows the equivalent block lateral dimensions versus the subvolume dimension for the thinnest layer, the thickest layer and all layers together. In layer 7, the most fractured layer, computed dimensions are within the range of 0.73 m to 0.92 m. These solutions are representative even for small section areas of less than 20 m x 20 m. On the contrary, in the least fractured layer, equivalent block dimension is considerably modified with subvolume lateral size. However it does not much change for subvolume dimension higher than 60 m. Therefore, the representativity of equivalent blocks results is directly related to the number of blocks in the section considered. For all layers together, the variations observed for layer 3 are attenuated but in a conservative approach, the R.E.V. of the equivalent block of a stack of layer should be fixed to the highest R.E.V. value of constitutive layers.

The equivalent block results for each layer of the complete image are given in **Table 2**. One can observe that the computed block size is correlated with the layer thickness, which is consistent with the correlation between fracture density and layer thickness used to generate this image.

The validity of the previous R.E.V. study assumes that the discretization of blocks into pixels is sufficient for each layer. The lateral pixel size used was equal to 4.47 cm. A sensitivity study of results to discretization was carried out for a subvolume of 60 m x 60 m. The range of pixel size examined was from 2.8 cm to 10 cm, which corresponds to a number of pixels of 500 000 to 5 000 000. **Fig. 13** shows the equivalent block dimensions of layers 3 and 7 versus the pixel size. It also gives the number of pixels used for the image discretization versus the pixel size. Whatever the layer considered, its equivalent block dimension slightly increases with the pixel size but this variation does not exceed 5%. Therefore, the equivalent block dimensions computed in the R.E.V. study are reliable for all layers, even the most fractured one (layer 7). Larger pixel sizes have been examined in order to find, for each layer, the limit beyond which the equivalent block dimension becomes unacceptable, that is, 20% higher than its real value (computed with a 2.8 cm pixel size). **Fig. 14** shows, for each layer, the limit point of which coordinates are the 20% overestimated block dimension and the corresponding pixel size. For the smallest equivalent block dimension, in layer 7, the limit pixel size is equal to 25 cm, which corresponds to a discretization of 160 000 pixels for the complete 100 m x 100 m image. The limit points referring to the 9 layers fit to a straight line of which slope corresponds to the discretization threshold of the representative block in any layer. This threshold is of 5 x 5 pixels per representative block of a given layer. For practical purposes, we may fix a limit of 10 x 10 pixels. This conservative limit value would give a number of 1 400 000 for the discretization of layer 7 in the 100 m x 100 m image, which is still less than the discretization adopted for the reported R.E.V. study.

## Conclusion

A new procedure, called the geometrical method, has been developed to compute the horizontal dimensions of Warren & Root equivalent blocks from fractured reservoir images. It is based on a simplified representation of the water-oil imbibition mechanism. Despite the assumptions underlying this representation, the geometrical method provides reliable solutions in terms of multiphase flow behavior. Furthermore, this fast procedure can be applied to large geological sections, in the order of magnitude of reservoir gridblocks. Further developments of the geometrical method are considered in order to take into account non vertical fractures, non conductive fractures and anisotropy of matrix permeability.

## Acknowledgments

This research program has been sponsored by an industrial consortium involving Aramco Overseas Company B.V., Elf Aquitaine Production, Enterprise Oil plc, Qatar General Petroleum Corporation and Total Exploration Production. The authors wish to acknowledge the members of this consortium for their technical and financial support.

## References

1. Warren, J.E. and Root, P.J.: "The Behavior of Naturally fractured reservoirs," *SPE Journal* (Sept. 1963),245-255.
2. Bourbiaux, B., Cacas M.C., Sarda S., Sabathier J.C.: "A fast and Efficient Methodology to Convert Fractured Reservoir Images Into a Dual Porosity Model," paper SPE 38907 presented at the 1997 SPE Annual Technical Conference and Exhibition, San Antonio, Texas, Oct. 5-8.
3. Bourbiaux, B. and Kalaydjian, F.: "Experimental study of Cocurrent and Countercurrent Flows in Natural Porous Media," *SPE Reservoir Engineering* (August 1990) 361-368.
4. Marle, C.M.: "*Multiphase flow in porous media*", Editions Technip, Paris (1981).
5. Mattax, C.C. and Kyte, J.R.: "Imbibition Oil Recovery From Fractured, Water-Drive Reservoir," *SPEJ* (June 1962) 177-184.
6. Cuiec, L., Bourbiaux, B. and Kalaydjian, F.: "Oil Recovery by Imbibition in Low-Permeability Chalk," *SPE Formation Evaluation* (Sept. 1994) 200-208.

Table 1: water-oil relative permeabilities and capillary pressures

Water saturation	Relative perm. to water	Relative perm. to oil	Capillary pressure (bar)
0.20	0.	0.80	2.30
0.25	0.0003	0.68	1.10
0.30	0.002	0.57	0.80
0.35	0.005	0.47	0.57
0.40	0.010	0.37	0.37
0.45	0.018	0.28	0.25
0.50	0.028	0.20	0.17
0.55	0.041	0.13	0.11
0.60	0.057	0.072	0.06
0.65	0.077	0.025	0.03
0.70	0.100	0.	0.

Table 2: Equivalent blocks in the demonstration image

Layer	Thickness (m)	Equivalent block size (m)
1	2.4	4.8
2	1.8	4.3
3	5.8	8.6
4	1.3	3.3
5	2.7	5.7
6	0.8	2.3
7	0.3	0.8
8	0.9	2.6
9	0.6	1.9
1 to 9	16.6	5.2

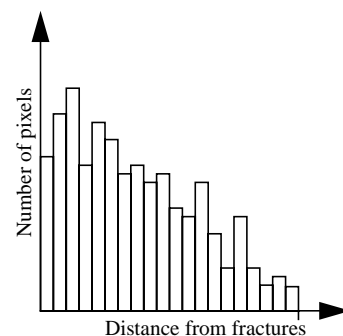


Fig. 1 - Histogram of pixels values

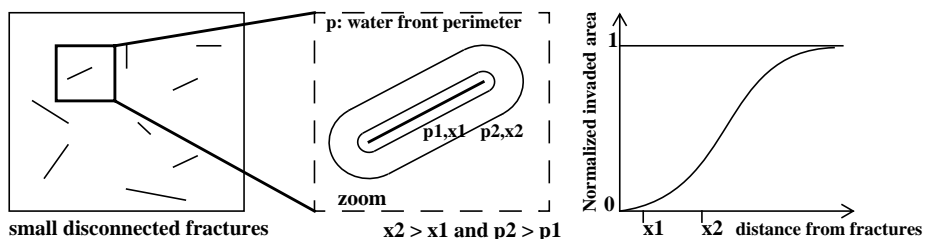


Fig. 2 - Increasing water front length in a layer with disconnected fractures

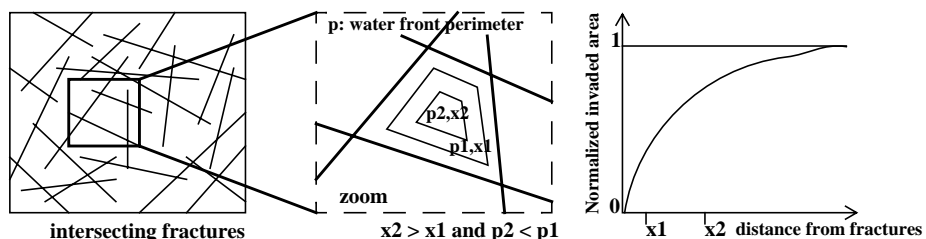


Fig. 3 - Decreasing water front length in a layer with well connected fractures

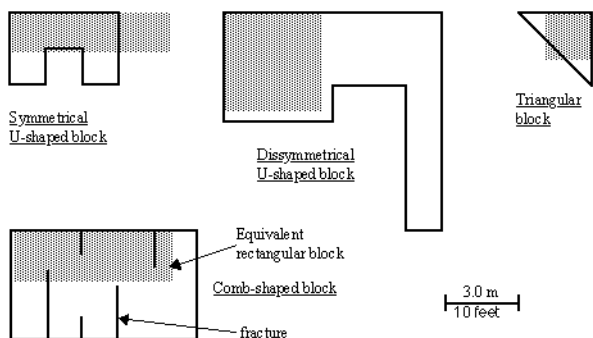


Fig. 4 - Single blocks considered to validate the geometrical method

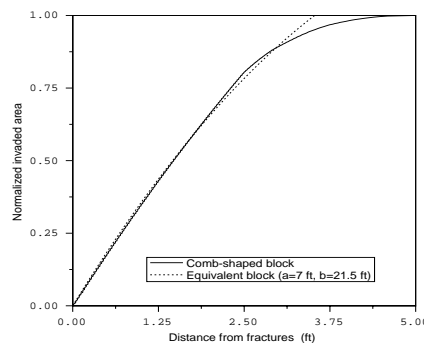


Fig. 5 - Area-distance curves of the comb-shaped block and the equivalent block

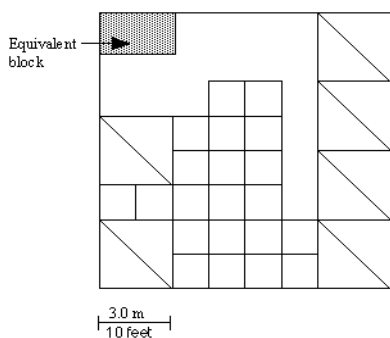


Fig. 7 - Distribution of square, triangular and U-shaped blocks

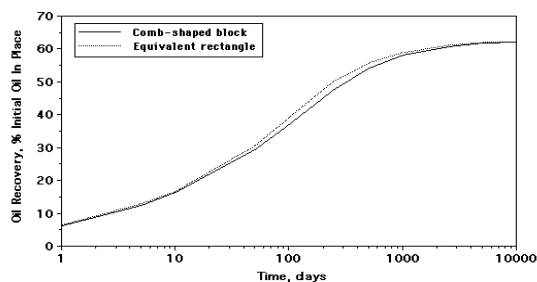
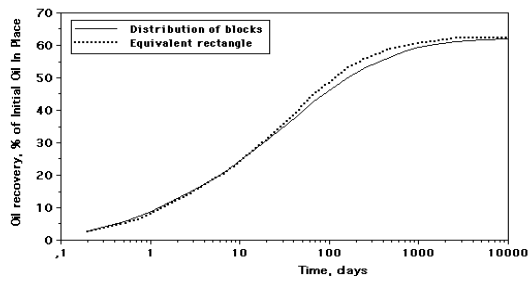
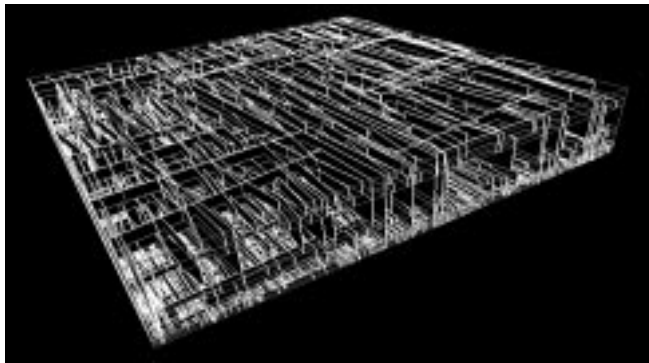


Fig. 6 - Water-oil imbibition in the comb-shaped block and the equivalent rectangular block



**Fig. 8 - Water-oil imbibition in the distribution of blocks and the equivalent rectangular block**



**Fig. 9 - 3D view of the demonstration image**

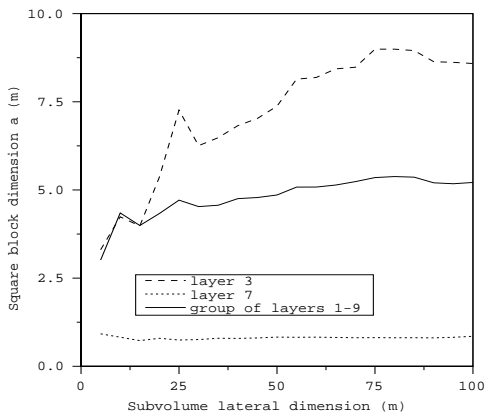


**Fig. 12 - Equivalent blocks in the demonstration image. Evolution with subvolume size.**

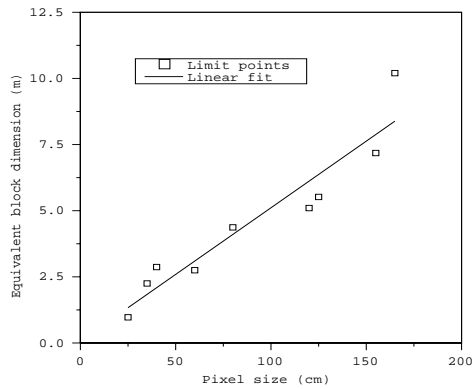


**Fig. 14 - Pixel size limit points of the 9 layers of the demonstration image and linear fit.**

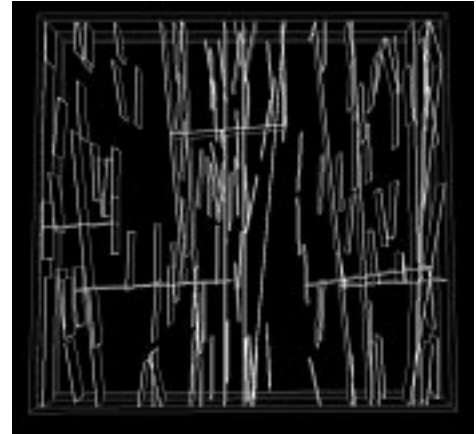


**Fig. 10 - Top view of Layer 3 in the demonstration image**

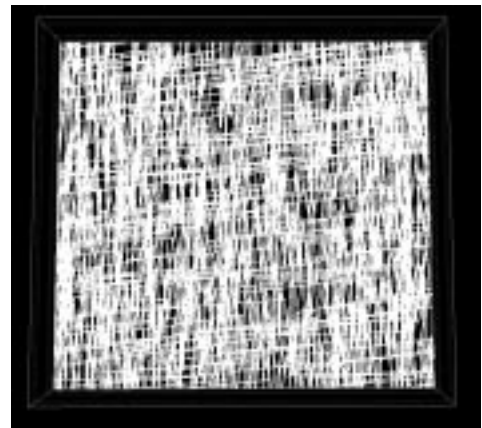


**Fig. 11 - Top view of Layer 7 in the demonstration image**

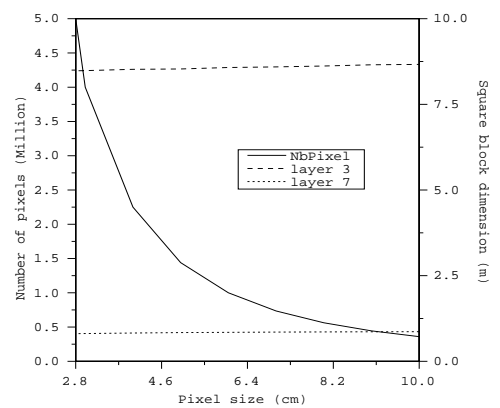


**Fig. 13 - Equivalent blocks in the demonstration image and number of pixels. Evolution with pixel size.**